

# Magnetic Single-Electron Transistor as a Tunable Model System for Kondo-Destroying Quantum Criticality

Stefan Kirchner<sup>a,\*</sup>, Qimiao Si<sup>a</sup>,

<sup>a</sup>*Department of Physics & Astronomy, Rice University, Houston, TX 77005, USA*

---

## Abstract

Single-electron transistors (SET) attached to ferromagnetic leads can undergo a continuous quantum phase transition as their gate voltage is tuned. The corresponding quantum critical point separates a Fermi liquid phase from a non-Fermi liquid one. Here, we expound on the physical idea proposed earlier. The key physics is the critical destruction of the Kondo effect, which underlies a new class of quantum criticality that has been argued to apply to heavy fermion metals. Its manifestation in the transport properties is studied through an effective Bose-Fermi Kondo model (BFKM); the bosonic bath, corresponding to the spin waves of the ferromagnetic leads, describes a particular type of sub-Ohmic dissipation. We also present results for general forms of sub-Ohmic dissipative bath, and consider in some detail the case with critical paramagnons replacing spin waves. Finally, we discuss some delicate aspects in the theoretical treatment of the effect of a local magnetic field, particularly in connection with the frequently employed Non-Crossing Approximation (NCA).

*Key words:* Single-electron transistor; Bose-Fermi Kondo model; quantum phase transitions; non-crossing approximation

*PACS:* 73.21.La, 71.10.Hf, 75.20.Hr, 71.27.+a

---

The term Kondo effect refers to the screening of a localized moment in a metallic host, a process that is mediated by particle-hole excitations of the host's itinerant electrons. The screened ground state is an entangled singlet between the local moment and the electrons, and the excitation spectrum contains a Kondo resonance which has the same quantum numbers as a bare electron. The possibility that quantum dots (QD), nanostructures with a well-defined local moment weakly interacting with nearby electrodes, could be used to model the Kondo effect was suggested early on [1,2].

Over the past decade, the Kondo effect has been realized in semiconductor heterostructures followed by nanotubes and single-molecule devices [3,4,5,6,7]. These developments have enhanced our understanding of the quantum impurity physics and lead to an increased interest in the formation of Kondo correlations in various settings, *e.g.* far away from thermal equilibrium [8,9]. Over roughly the same period, studies in the bulk correlated systems of heavy fermion metals have focused attention on quantum critical points (QCP). Historical work in heavy fermions addressed the heavy Fermi liquid on one hand [10], and

the competition between Kondo and RKKY interactions on the other [11,12]. The recent studies have instead centered around the critical destruction of the Kondo effect on the verge of an antiferromagnetic ordering at zero temperature [13,14,15,16]. It is natural to ask whether related effects can be realized in nanostructures.

We recently showed that a single-electron transistor (SET) attached to ferromagnetic leads [17] constitutes a tunable quantum impurity model system for a Kondo-destroying QCP. The purpose of this article is, in addition to reviewing the basic physical idea and some salient results on this setup, addressing two issues. First, we determine what happens when spin waves are replaced by critical paramagnons; these results will be relevant when the ferromagnetic leads are replaced by, for instance, palladium, which maybe better suited to form SET structures with certain molecules [18]. Second, we discuss some methodological issues that arise when considering the effect of a local magnetic field.

## 1. Quantum Criticality in a Ferromagnetic SET

The general setup of the magnetic SET is given in Fig. 1a. The magnetic excitation spectrum of an itinerant

---

\* Corresponding author. Tel: (713) 348-4291 fax: (713) 348-4150  
Email address: kirchner@rice.edu (Stefan Kirchner).

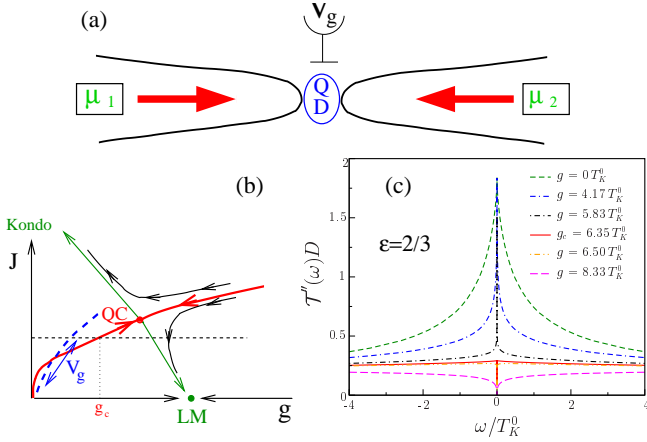


Fig. 1. (a) Schematics of the ferromagnetic SET. The red arrows label the lead magnetization and  $\mu_i$ ,  $i = L, R$  the chemical potential in the L/R lead coupled to the quantum dot QD. (b) Phase diagram of the low-energy model of the ferromagnetic SET. Varying the gate voltage  $V_g$  tunes both, the Kondo ( $J$ ) and the spin wave coupling ( $g$ ) along the dashed (blue) line. The dotted horizontal line is the path across the transition in Figs. 1c and 2. (c) Evolution of the Kondo resonance, for  $\epsilon = 2/3$ , the case of critical paramagnons. The continuous (red) red curve is at the critical coupling,  $g = g_c$ . The parameters adopted are:  $J = 0.8D$ , where  $D$  is the bandwidth associated with  $E_{\mathbf{k}}$ , and correspondingly  $T_K^0 = 0.06D$ ; the cut-off energy for the bosonic bath is  $\Lambda = 0.32D$ .

ferromagnet consists of the Stoner continuum, i. e. triplet particle-hole excitations, and spin waves. Given the Zeeman-splitting of the bands, it might at first be surprising that ferromagnetic leads can screen the local moment. The important point is that the local moment is coupled to all possible particle-hole combinations of both the source and drain leads. The resulting exchange coupling matrix is such that the anti-symmetric combination of the two leads decouple from the local moment [1,2]:

$$\mathbf{J} \sim \begin{pmatrix} V_L^* V_L & V_L^* V_R \\ V_L V_R^* & V_R^* V_R \end{pmatrix} = \mathcal{U} \begin{pmatrix} V_L^* V_L + V_R^* V_R & 0 \\ 0 & 0 \end{pmatrix} \mathcal{U}^\dagger, \quad (1)$$

where  $V_i$  is the hybridization strength to the left/right ( $i = L/R$ ) lead and the proportionality factor depends on the charging energy of the dot and the chemical potential of source and drain. The local moment hence couples to the sum of the DOS of both leads. If the magnetization in the source and drain are anti-aligned and the SET setup is otherwise symmetric w.r.t. the two leads, the local moment couples to an effective band of unpolarized electrons and complete Kondo screening is recovered for arbitrary spin polarization in the leads [19]. This was experimentally verified by Pasupathy et al. [20]. Here, to illustrate the basic physics, we will focus on such an anti-parallel case.

The new observation we introduced in Ref. [17] is not that Stoner excitations can screen the local moment but that the spin waves in the ferromagnetic leads will also couple to it. The derivation of the effective low-energy model, given in Ref. [17], confirms this symmetry argument. A generalized Schrieffer-Wolff transformation yields the following

effective low-energy Hamiltonian [17]:

$$\mathcal{H}_{\text{bflk}} = J \sum_i \mathbf{S} \cdot \mathbf{s}_i + \sum_{\mathbf{k}, i, \sigma} \tilde{\epsilon}_{\mathbf{k}\sigma i} c_{\mathbf{k}\sigma i}^\dagger c_{\mathbf{k}\sigma i} + h_{\text{loc}} S_z + g \sum_{\beta, \mathbf{q}, i} S_\beta (\phi_{\beta, \mathbf{q}, i} + \phi_{\beta, \mathbf{q}, i}^\dagger) + \sum_{\beta, \mathbf{q}, i} \omega_{\mathbf{q}} \phi_{\beta, \mathbf{q}, i}^\dagger \phi_{\beta, \mathbf{q}, i}. \quad (2)$$

where the local magnetic field  $h_{\text{loc}} = g \sum_i m_i$ , with  $m_i$ , for  $i = L, R$ , being the ordered moment of the left/right leads,  $\tilde{\epsilon}_{\mathbf{k}\sigma i}$  is the Zeeman-shifted conduction electron dispersion, and  $\phi_{\beta, i}$ , with  $\beta = x, y$ , describes the magnon excitations. With the canonical transformation, Eq. (1), for the fermionic bath and a similar one for the bosonic bath, the effective fermionic dispersion, labeled  $E_{\mathbf{k}}$ , becomes spin-independent; moreover, the antisymmetric combinations of each bath decouple. Hence, the low-energy properties of the ferromagnetic SET are governed by a BFKM with an easy-plane anisotropy. For the anti-parallel alignment,  $m_L = -m_R$ , and  $h_{\text{loc}}$  will vanish.

Magnons are gapless bosons with a quadratic dispersion. The spectral density of the local dissipation they generate is sub-Ohmic,

$$\int dq^3 \delta(\omega - \omega_q) \sim \sqrt{\omega}. \quad (3)$$

This feature turns out to be essential for the existence of a QCP [21]. Fig. 1b shows the corresponding phase diagram of the ferromagnetic SET. There are three renormalization-group fixed points: “Kondo” and “LM” refer to the Kondo screened Fermi-liquid fixed point, and the critical local-moment fixed point, describing a quantum-critical phase. “QC” refers to the quantum-critical fixed point, characterizing the critical Kondo screening on the entire separatrix (red line, corresponding to the critical coupling  $g_c$  as a function of  $J$ ). Most dissipation channels will not lead to sub-Ohmic fluctuation spectra; coupling to phonons, photons, or antiferromagnetic magnons will not lead to critical Kondo screening.

The generalized Schrieffer-Wolff transformation relates the coupling constants  $J$  (Kondo coupling) and  $g$  (magnon coupling) of Eq. (2) to the coupling constants of the original model:  $J \sim \Gamma/(\rho\Delta)$  and  $g \sim \Gamma/(\rho\Delta)^2$ , where  $\Gamma = \pi\rho V^2$  is the hybridization width, and  $\rho$  is the lead density of states at the Fermi energy.  $\Delta$  is the charge fluctuation energy and is linearly dependent on the gate voltage  $V_g$  of the SET. The gate voltage is therefore able to tune the competition between the Kondo coupling and the coupling to the fluctuating magnon field. Since the Kondo screening occurs on the scale of the bare ( $g = 0$ , no magnons) Kondo temperature  $T_K^0 = (1/\rho) \exp(-1/\rho J)$ , the control parameter is  $g/T_K^0$ .  $T_K^0$  depends exponentially on  $J$ , whereas  $g \sim J^2$ . This implies that  $g/T_K^0$  is exponentially large deep in the Kondo regime and becomes of order unity in the mixed valence regime. This situation is reminiscent of the so-called Doniach-Varma picture for the Kondo lattice where the RKKY interaction ( $\sim J^2$ ) competes with the Kondo singlet formation ( $\sim T_K^0$ ) [11]. This analogy is not accidental.

The quantum phase transition as  $g$  is tuned through  $g_c$  is reflected in the narrowing of the Kondo resonance, as seen in Fig. 1c. The transport properties in the quantum critical regime have been worked out in Ref. [17]. In the Kondo phase the conductance has the well-known Fermi-liquid form,  $G(T) = a - bT^2$ , where  $a = 2e^2/h$  follows from Friedel's sum rule. In the critical local moment phase ( $g > g_c$ ) at  $T = 0$ , the electrons are completely decoupled from the local moment and the conductance vanishes. At finite temperatures, we find  $G(T) = cT^{1/2}$ . The conductance versus temperature at the critical gate voltage shows fractional power-law behavior,  $G(T) = A + BT^{1/4}$ , where  $A$  is smaller than  $a$ . The experimental feasibility of these measurements has been extensively discussed in Ref. [17].

We now make the connection between our results and the physics of quantum critical heavy fermion systems. The BFKM has been put forth as an effective model for a Kondo-destroying QCP in heavy fermion systems [13]. In this approach, the self-consistency relation between the lattice system and the effective impurity model gives rise to a sub-Ohmic spectrum. The inference about the destruction of Kondo effect at the antiferromagnetic QCP of heavy fermion systems have come from the collapse of a large Fermi surface and the vanishing of multiple energy scales [15,16]. The ferromagnetic SET structure discussed here provides a tunable model system to study the physics of a critical destruction of Kondo effect.

## 2. The Case of Critical Paramagnons

If the leads contain critical paramagnons instead of spin waves, the dynamical spin susceptibility of the leads will have an over-damped form:

$$\chi_{\text{leads}}(\mathbf{q}, \omega) \sim \frac{1}{q^2 - i\omega/\gamma q} \quad (4)$$

where  $\gamma$  is a constant. The dissipative spectrum becomes

$$\int dq^3 \text{Im}\chi_{\text{leads}}(\mathbf{q}, \omega) \sim |\omega|^{1/3} \text{sgn}(\omega). \quad (5)$$

Since in this case the spin-rotational invariance in the leads is not broken, the issue of anti-parallel alignment does not arise. Palladium, for instance, has a Stoner enhancement factor of around 10; there will be a large frequency window over which Eq. (5) applies. Furthermore, contact properties of palladium leads are well studied and seem to be characterized by a relatively small contact resistance [22]. It has been argued [17] that temperature/frequency dependences of the critical electronic properties of BFKM with easy-plane anisotropy are similar to those of the same model with SU(2) invariance. For the Kondo-destroying QCP and the critical local-moment phase, it was further argued that they are similar to those of a large-N limit of an SU(N)  $\times$  SU(N/2) generalization of the BFKM:

$$\mathcal{H}_{\text{BKF}} = (J/N) \sum_{\alpha} \mathbf{S} \cdot \mathbf{s}_{\alpha} + \sum_{\mathbf{k}, \alpha, \sigma} E_{\mathbf{k}} c_{\mathbf{k}\alpha\sigma}^{\dagger} c_{\mathbf{k}\alpha\sigma}$$

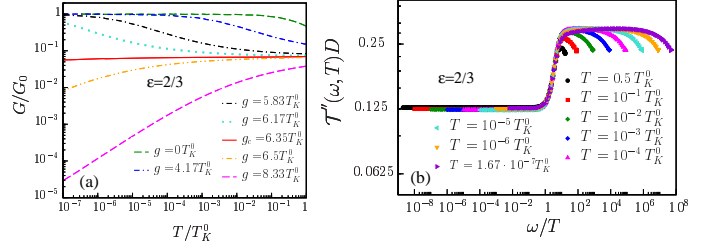


Fig. 2. (a) DC conductance for different coupling strengths  $g$ , for  $\epsilon = 2/3$ , the case of critical paramagnons. The zero temperature value of the conductance in the Fermi liquid vase is fixed through the Friedel-Langreth sum rule. (b)  $\omega/T$ -scaling at the QCP ( $g = g_c$ ). The universal scaling curve of the T-matrix can be probed via the AC conductance and Johnson noise measurements [17].

$$+ (g/\sqrt{N}) \mathbf{S} \cdot \Phi + \sum_{\mathbf{q}} \omega_{\mathbf{q}} \Phi_{\mathbf{q}}^{\dagger} \cdot \Phi_{\mathbf{q}}. \quad (6)$$

The large-N limit leads to a set of dynamical saddle-point equations [25], which can be solved analytically at zero temperature and numerically at finite temperatures.

Alternatively, the dynamical equations, exact in the large-N limit, can be used as an approximation for the  $N = 2$  case. Ref. [17] considered the  $N = 2$  version of the Bose-Fermi Anderson model,

$$H_{\text{bfam}} = \sum_{\mathbf{k}, \sigma} E_{\mathbf{k}} c_{\mathbf{k}\sigma}^{\dagger} c_{\mathbf{k}\sigma} + t \sum_{\mathbf{k}, \sigma} \left( c_{\mathbf{k}\sigma}^{\dagger} d_{\sigma} + \text{h.c.} \right) + \varepsilon_d \sum_{\sigma} d_{\sigma}^{\dagger} d_{\sigma} + U n_{d\uparrow} n_{d\downarrow} + g \mathbf{S}_d \cdot \Phi + \sum_{\mathbf{q}} \omega_{\mathbf{q}} \Phi_{\mathbf{q}}^{\dagger} \cdot \Phi_{\mathbf{q}}, \quad (7)$$

at  $U = \infty$  (and, hence, particle-hole asymmetric). The numerical results presented in Ref. [17] are all for this  $N = 2$  case. At zero field, they have the same behavior as the exact results in the large-N limit of Eq. (6).

We observe that the dissipative spectrum associated with the critical paramagnons, Eq. (5), can be cast into the general form considered in Ref. [25],

$$A_{\Phi}(\omega) \sim |\omega|^{1-\epsilon} \text{sgn}(\omega), \quad (8)$$

with  $\epsilon = 2/3$ . For general  $\epsilon$ , the large-N results at zero temperature [25] imply that, for the critical point ( $g = g_c$ ),

$$T''(\omega > 0) = \text{const}_1 + \text{const}_2 \cdot \omega^{\epsilon/2}. \quad (9)$$

Likewise, for the critical local-moment phase ( $g > g_c$ ),

$$T''(\omega > 0) = \text{const} \cdot \omega^{\epsilon}. \quad (10)$$

For the case appropriate to critical paramagnons,  $\epsilon = 2/3$ , we have carried out more detailed studies based on the large-N limit of Eq. (6). Fig. 1c demonstrates the destruction of Kondo resonance as the dissipative coupling  $g$  reaches  $g_c$  and beyond. The DC conductance as a function of temperature is given in Fig. 2a. The temperature exponent at  $g = g_c$  and  $g > g_c$  are compatible to  $1/3$  and  $2/3$  respectively. The equality of these exponents with their counterparts in the  $T = 0$  frequency dependence is consistent with  $\omega/T$  scaling. The latter is further illustrated in

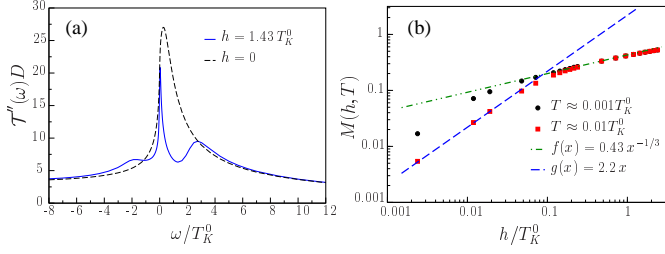


Fig. 3. (a) Kondo resonance in zero (dashed line) and finite local field (continuous line). The NCA, while capturing the Zeeman-split peaks, incorrectly produces a sharp resonance that is pinned to the Fermi energy ( $\omega = 0$ ). This reflects its failure to capture the marginally irrelevant character of the potential scattering term. (b) Local magnetization at the critical coupling  $g_c$ . The results are consistent with the expectation based on hyperscaling. The parameters adopted are:  $\epsilon_d = -0.3D$ ,  $U = \infty$ ,  $t = 0.1D$ , corresponding to  $T_K^0 = 4.2 \times 10^{-3}D$ ; the cut-off energy for the bosonic bath  $\Lambda = 0.32D$ .

Fig. 2b, which demonstrates the  $\omega/T$  scaling collapse of the dynamical T-matrix at  $g = g_c$ . This  $\omega/T$  scaling provides evidence for the interacting nature of the QCP. Because  $\epsilon > 1/2$ , the latter in turn is an indication for an unconventional quantum criticality [25,26,27].

### 3. Issues on NCA in a finite field

In the case of ferromagnetic leads, a local magnetic field will arise if the ordered moments of the two leads are parallel, or if the couplings to the leads are asymmetric in the anti-parallel configuration. This refers to  $h_{\text{loc}}$  of Eq. (2), along the direction of magnetic ordering. The effect of this field goes beyond Eqs. (6,7). In the following, we briefly discuss what would happen if we were to incorporate a local field in Eqs. (6,7). This effect is relevant if an external local field is applied along any of the spin-wave directions in the ferromagnetic case, or along any direction in the case of critical paramagnons. We further restrict to the case of Eq. (7), where for  $g = 0$  the large- $N$  equations reduce to the commonly applied NCA formalism. Our purpose is to illustrate some delicate aspects in the theoretical treatment of such a local field,  $h$ .

The Kondo effect ( $g = 0$ ) in the presence of a magnetic field is a well-studied subject [23]. The poor performance of the NCA for this problem has, however, not been extensively discussed in the literature. It was shown in Ref. [24] that within the NCA the potential scattering term of the Anderson model *incorrectly* scales in the same manner as the spin exchange coupling. In a magnetic field, the up and down fermions will be Zeeman-split. This gives rise to the splitting of the Kondo resonance which is reproduced by the NCA, see Fig. 3a. The NCA does however overestimate the asymmetry of the two peaks and, more significantly, it incorrectly predicts a sharp feature at the Fermi energy ( $\omega = 0$ ). This sharp resonance is due to the NCA's incorrect treatment of the potential scattering term. Since this term is not affected by the local field, the 'Kondo resonance' due to this term remains at  $\omega = 0$ .

At the QCP, on the other hand, the Kondo effect has been destroyed. One might therefore expect that the NCA can still be used to obtain universal properties at a finite local field. Following a hyperscaling analysis similar to that given in Ref. [28], and using the fact that  $\chi_{\text{stat}} \sim T^{\epsilon-1}$ , we find that, for  $\epsilon = 1/2$ ,

$$M(h, T = 0) \sim |h|^{\epsilon/(2-\epsilon)} = |h|^{1/3}, \quad (11)$$

and we expect  $|h|/T^{(2-\epsilon)/2} = |h|/T^{3/4}$ -scaling. For  $h \ll T$  the magnetization should therefore behave as  $M(h, T) \sim |h|$ , whereas for  $h \gg T$  it will be  $M(h, T) \sim |h|^{1/3}$ . (We have set  $g\mu_B = 1$ .) This behavior is correctly reproduced by the NCA, see Fig. 3b. We conclude that the NCA, generalized to incorporate the coupling to the bosonic bath, correctly captures certain universal properties of the quantum critical BFKM in a finite local field.

In conclusion, a SET with ferromagnetic electrodes constitutes a tunable spintronic system that allows to experimentally access a quantum critical Kondo state. Nonequilibrium properties of this boundary quantum phase transition are readily obtained by having  $\mu_1 \neq \mu_2$  [see Fig. 1a]. The ferromagnetic SET therefore seems to be an ideal system to address out-of-equilibrium aspects of quantum criticality both theoretically and experimentally.

This work was supported in part by NSF, the Robert A. Welch Foundation, the W. M. Keck Foundation, and the Rice Computational Research Cluster funded by NSF, and a partnership between Rice University, AMD and Cray.

### References

- [1] L. I. Glazman and M. E. Raikh, JETP Lett. 47 (1988) 452.
- [2] T. K. Ng and P. A. Lee, Phys. Rev. Lett. 61 (1988) 1768.
- [3] D. Goldhaber-Gordon et al., Nature 391 (1998) 156.
- [4] J. Nygard et al., Nature 408 (2000) 342.
- [5] J. Park et al., Nature 417 (2002) 722.
- [6] W. Liang et al., Nature 417 (2002) 725.
- [7] L. H. Yu and D. Natelson, Nano Letters 4 (2004) 79.
- [8] J. Paaske et al., Nature Physics 2 (2006) 460.
- [9] B. Doyon and N. Andrei, Phys. Rev. B 73 (2006) 245326.
- [10] A. Hewson, *The Kondo Problem to Heavy Fermions*, Cambridge University Press (1993).
- [11] S. Doniach, Physica B 91 (1977) 231.
- [12] C. M. Varma, Rev. Mod. Phys. 48 (1976) 219.
- [13] Q. Si et al., Nature 413 (2001) 804.
- [14] P. Coleman et al., J. Phys. Cond. Matt. 13 (2001) R723.
- [15] S. Paschen et al., Nature 432 (2004) 881.
- [16] P. Gegenwart et al., Science 315 (2007) 969.
- [17] S. Kirchner et al., Proc. Natl. Acad. Sci. USA 102 (2005) 18824.
- [18] D. Natelson, private communication.
- [19] J. Martinek et al., Phys. Rev. Lett. 91 (2003) 247202.
- [20] A. N. Pasupathy et al. Science 306 (2004) 86.
- [21] L. Zhu and Q. Si, Phys. Rev. B 66 (2002) 024426; G. Zarand and E. Demler, *ibid.* (2002) 024427.
- [22] B. Babic and C. Schönenberger, Phys. Rev. B 70 (2004) 195408.
- [23] T. A. Costi, Phys. Rev. Lett. 85 (2000) 1504.
- [24] S. Kirchner and J. Kroha, J. Low Temp. Phys. 126 (2002) 1233.
- [25] L. Zhu et al., Phys. Rev. Lett. 93 (2004) 267201.
- [26] M. Vojta et al., Phys. Rev. Lett. 94 (2005) 070604.

- [27] M. Glossop and K. Ingersent, Phys. Rev. Lett. 95 (2005) 067202.
- [28] K. Ingersent and Q. Si, Phys. Rev. Lett. 89 (2002) 076403.